Numerical evidence of stationary and breathing concentration patterns in the Oregonator with equal diffusivities

Jack D. Dockery*
Department of Mathematical Sciences, Montana State University, Bozeman, Montana 59715

Richard J. Field†
Department of Chemistry, The University of Montana, Missoula, Montana 59812

(Received 2 September 1997)

The set of three reaction-diffusion equations describing the time-space behavior of the intermediate chemical species in the Oregonator model of the Belousov-Zhabotinsky reaction is investigated in an open, gel-disk reactor in one and two spatial dimensions. Numerical simulations using equal values of the three diffusion coefficients indicate the presence of solutions corresponding to large-amplitude, apparently stable, stationary concentration patterns. The requirement of differential transport rates of chemical activator and inhibitor species for the development of stable patterns is apparently met in this system by differential exchange rates with the reservoir(s) rather than by differential diffusion rates within the gel-reactor. The characteristics of these patterns as well as their stability and bifurcation properties are investigated and suggest that their appearance is dependent upon the existence of bistability in the homogeneous reaction kinetics. The patterns have an intrinsic wavelength, and one of a particular wave-number destabilizes via a Hopf bifurcation as the length of the gel-reactor is varied, giving rise to oscillatory breather-solutions past the bifurcation but before decomposition into a spatially homogeneous state occurs. The relationship of these results to experimental systems, as well as an analogy to the behavior of biological membranes, is discussed.
[S1063-651X(98)13407-4]

PACS number(s): 82.70.−y

I. INTRODUCTION

A. M. Turing [1,2] suggested in 1952 that the interaction of reaction and diffusion of intermediate species in spatially distributed, convection-free, reacting chemical systems may lead under appropriate conditions to spontaneous destabilization of the spatially homogeneous steady state and formation of temporally stable, spatially inhomogeneous patterns in the concentrations of these species. The resulting patterns are characterized by an intrinsic spatial wavelength that is determined by the reaction-diffusion dynamics of the system rather than by its geometry.

The required conditions [3] are (i) the system is maintained far from chemical equilibrium [4], (ii) the chemical kinetics is of the activator-inhibitor type [2,5,6], and (iii) the diffusion coefficient of the inhibitor species is larger than that of the activator species by an amount related to the chemical parameters of the system [2,3]. This difference in diffusion coefficients is difficult to achieve in simple chemical systems in which most species diffuse at similar rates.

Stationary concentration patterns in principle can be stabilized indefinitely in an open [continuous-flow, unstirred reactor (CFUR)] system where the distance from chemical equilibrium is maintained by the exchange of reactants and products with reservoir(s) while the overall chemical reaction occurs [7]. The chemical reaction occurs in a gelled medium to avoid convective effects. Both the existence of stable patterns and the bifurcation structure of the dynamical system are dependent upon CFUR flow rates and other parameters, e.g., the physical dimensions of the open reactor.

The activator species [2,5,6] is one that is formed in an autocatalytic process, and the inhibitor species is one that is derived from the activator but has the effect of inhibiting the autocatalytic formation of the activator. Such systems normally will be bistable for at least some values of the chemical concentrations and rate constants; one state features high activator and low inhibitor concentrations, while the other features low activator and high inhibitor concentrations. Oscillations often may occur between these two states.

The stabilizing effect on concentration patterns of the higher transport-rate (e.g., diffusion coefficient or exchange-rate with a reservoir) of the inhibitor relative to the activator may be understood in the following way. Consider a localized area in which the activator is being autocatalytically formed and is subsequently leading to formation of the inhibitor species. Autocatalytic formation of the activator is not occurring in the surrounding area. If the transport rate of the inhibitor out of this local area is sufficiently low, then its concentration will eventually rise to the point where it stops autocatalytic formation of the activator. However, if the rate of transport of the inhibitor out of the activated area is sufficiently high relative to that of the activator, then activator production continues indefinitely. Furthermore, rapid transport of inhibitor into the surrounding area keeps it inactive. The combination of these two effects stabilizes the localized area of activation as well as its surrounding inhibited area.

Nearly 40 years elapsed between Turing's suggestion [1] and its first experimental verification by Castets *et al.* [8] and shortly afterward by Ouyang and Swinney [9] because of the necessary development of both appropriate chemical reactions [10,11] and suitable CFUR experimental arrangements

*Electronic address: umsfjdoc@math.montana.edu
†Electronic address: ch_rjf@selway.umt.edu

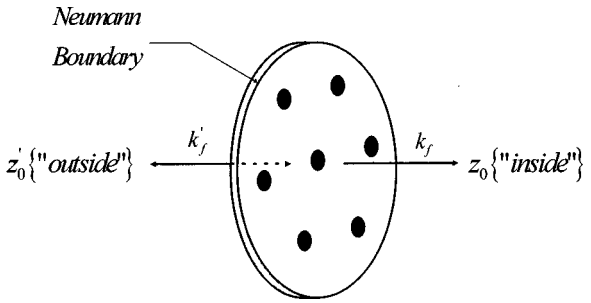

FIG. 1. Schematic diagram of a gel-disc reactor showing the thin-layer reaction medium in contact with two reservoirs and associated transport parameters, k_f, k_f', z_0, and z_0'. Only one reservoir is considered in this work.

[7,12,13,14]. The chlorite-iodide-malonic acid (CIMA) system [15,16] is used in these experiments in which a gelled-CFUR is fed the appropriate chemicals from reservoirs. The required difference in diffusion rates is obtained [16] by using a gel containing immobilized starch in order to decrease the effective diffusion-rate of the chemically coupled activator species $I^-/I_2/I_3^-$ by complexing I_3^-.

Several gel-CFUR/reservoir configurations have been used in the CIMA system, including the thin-strip reactor [8,17,18], the gel-disc reactor [9,19,20], and the beveled-gel reactor [21]. The analysis and calculations reported here apply to a gel-disk reactor, shown schematically in Fig. 1, which consists of a very thin circle of gel of diameter L sandwiched between reservoir(s) in contact with one or both faces. The transport processes involving chemical species are diffusion within the approximately two-dimensional gel itself and exchange between the gel-CFUR and the reservoir(s). All points within the gel are in contact with the reservoir(s), and there are no concentration gradients within the gel-reactor imposed by reservoir configuration, assuming the gel to have no thickness. Concentration patterns develop within the plane of the gel.

Unambiguous experimental evidence of reaction-diffusion-supported stationary concentration patterns has been obtained to our knowledge only in the CIMA and the $Fe(CN)_6^{4-}-IO_3^--SO_3^{2-}$ [15,16] systems. In particular, no experimental evidence has been obtained in the chemically and mechanistically well-understood [22–24] Belousov-Zhabotinsky (BZ) reaction [25–27], whose kinetics are of an activator-inhibitor nature and in which traveling concentration pattern experimental [28–31] and theoretical [32] work are well developed. The relationship between stationary and traveling concentration patterns has been investigated in the CIMA system [33]. Traveling concentration patterns are the expected phenomenon when diffusion rates are nearly equal, but no way has yet been found in the BZ system to achieve experimentally the required diffusion-rate difference between activator and inhibitor species for the appearance of stationary patterns. Such patterns, however, have been found numerically in the Oregonator model [34,35] of the BZ chemical dynamics in a closed system with constant reactant concentrations and unequal diffusion coefficients [36–39]. This state of affairs is unfortunate because the BZ reaction is well suited to experimental work with spatial concentration inhomogeneities. It is very robust and reproducible with sharply autocatalytic kinetics leading to well-defined patterns, and its mechanism is well understood, making the connection between experiment and the governing dynamic law clear.

The present work suggests that it may be possible in a gel-disk reactor to adjust the BZ reaction exchange rates between the CFUR-gel and its reservoirs so as to achieve, even with equal diffusion coefficients, the differential transport rate of activator and inhibitor required for stationary concentration pattern formation. The results obtained imply that stable patterns can be obtained only if concentrations and flow rates are adjusted such that the homogeneous kinetics, including the flow, are bistable. Furthermore, the stable patterns located do not bifurcate directly from the spatially homogeneous state and thus can be realized only through an appropriate perturbation, perhaps photochemical, of that state. Experimental verification of the predicted stable but oscillatory (breather) patterns, apparently related to the presence of a Hopf bifurcation in the partial differential equations, is to hoped for.

II. MODEL EQUATIONS

The Belousov-Zhabotinsky (BZ) reaction [25–27] in the form used in spatial-pattern work usually is composed of bromate ion $\{BrO_3^-\}$, malonic acid $\{CH_2(COOH)_2\}$, and a metal-ion catalyst $\{Fe(phen)_3^{3+}/Fe(phen)_3^{2+}\}$ in an ≈ 1 M sulfuric acid $\{H_2SO_4\}$ medium. The overall chemical reaction is the metal-ion catalyzed oxidation of malonic acid by bromate ion. The chemical mechanism of the BZ reaction was elucidated by Field, Körös, and Noyes [22] in 1972. This very complex mechanism involving in one form [24] 26 chemical species and 80 chemical reactions can be reduced to the five-reaction, three-variable model referred to as the Oregonator [34,35] given below:

$$A + Y \xrightarrow{k_1} X + P, \tag{1}$$

$$X + Y \xrightarrow{k_2} P + P, \tag{2}$$

$$A + X + C \xrightarrow{k_3} X + X + Z, \tag{3}$$

$$X + X \xrightarrow{k_4} A + P, \tag{4}$$

$$Z \xrightarrow{k_5} fY. \tag{5}$$

The chemical identities are $A \equiv BrO_3^-$, $P \equiv HOBr$, $X \equiv HBrO_2$, $Y \equiv Br^-$, $C \equiv Fe(phen)_3^{2+}$, and $Z \equiv Fe(phen)_3^{3+}$. The higher concentrations of BrO_3^- and HOBr, assumed to be the principal reactant and product, respectively, are held constant in a CFUR by transfer from the reservoirs, leaving the lower-concentration, intermediate species: $HBrO_2$, Br^-, and $Fe(phen)_3^{3+}$, as the dynamic variables. These lower-concentration species also exchange with the reservoirs, and the exchange rates of Br^- and $Fe(phen)_3^{3+}$ may be affected by their reservoir concentrations. $HBrO_2$ is not stable enough to be present in a reservoir. The conservation of Fe atoms for the two forms of the metal-ion catalyst [37,40] requires that C_{tot}=total concentration of metal ion=$[Fe(phen)_3^{3+}]$

$+[\mathrm{Fe(phen)_3}^{2+}]$. The values of k_1-k_4 are experimentally defined [34,35], while the values of k_5 and the stoichiometric factor f are treated as parameters. The value of $[\mathrm{CH_2(COOH)_2}]$ is absorbed into k_5. The kinetic parameters [37] used here are $k_1=2.5\,[\mathrm{H^+}]^2\mathrm{M^{-3}\,s^{-1}}$, $k_2=3.0\times10^6\,[\mathrm{H^+}]\,\mathrm{M^{-2}\,s^{-1}}$, $k_3=40\,[\mathrm{H^+}]\,\mathrm{M^{-2}\,s^{-1}}$, $k_4=3.0\times10^3\,\mathrm{M^{-1}\,s^{-1}}$, $k_5=0.10\,\mathrm{s^{-1}}$, $[\mathrm{H^+}]=0.8$ M, $[A]=0.06$ M, $C_{\mathrm{tot}}=2.3\times10^{-3}$ M, and $f=0.43$.

Using the scaled concentrations, x, y, z, and c defined by

$$x=(k_1A/k_2)/[X],\quad y=(k_3A/k_2)/[Y],$$

$$z=\{k_1k_3A^2/(k_2k_5)\}/[Z],$$

and

$$c=\{k_1k_3A^2/(k_2k_5)\}/[C_{\mathrm{tot}}],$$

and the dimensionless parameters s, q, w, and t defined by

$$s=(k_3/k_1)^{1/2},\quad q=2k_1k_4/k_2k_3,\quad w=k_5/(A\{k_1k_3\}^{1/2})$$

and

$$t=\mathrm{Time}\{A(k_1k_5)^{1/2}\},$$

the mass-action, well-mixed, spatially homogeneous chemical-kinetics equations become

$$\begin{aligned} dx/dt&=f(x,y,z)=s[y-xy+x(1-z/c)-qx^2],\\ dy/dt&=g(x,y,z)=(-y-xy+fz)/s,\\ dy/dt&=h(x,z)=w[x(1-z/c)-z]. \end{aligned}\tag{6}$$

Addition of Fick's Law diffusion terms within the gel and the scaled flow term, k_f, for the transfer of X, Y, and Z between the gel-CFUR and the reservoir(s) (Fig. 1) leads to Eq. (7),

$$\begin{aligned} \frac{\partial x}{\partial t}&=D\,\frac{\partial^2x}{\partial r^2}+f(x,y,z)-k_fx,\\ \frac{\partial y}{\partial t}&=D\,\frac{\partial^2y}{\partial r^2}+g(x,y,z)-k_fy,\\ \frac{\partial z}{\partial t}&=D\,\frac{\partial^2z}{\partial r^2}+h(x,z)+k_f(z_r-z). \end{aligned}\tag{7}$$

The additional scalings $D=D'/[A(k_1k_5)^{1/2}L^2]$ with $D'=1.0\times10^{-5}$ cm^2/s and $r=r'/L$ are introduced in Eq. (7) with the spatial coordinate r' and the reactor length L in cm. The scaled spatial coordinate r runs between 0 and 1 in these calculations with Neumann (no-flux) boundary conditions imposed at the endpoints. The parameter z_r is the reservoir concentration of Z. It is assumed that $x_r=y_r=0$.

We seek stable, spatially inhomogeneous solutions to Eq. (7), i.e., solutions to Eq. (8),

$$\begin{aligned} D\,\frac{\partial^2x}{\partial r^2}+f(x,y,z)-k_fx&=0,\\ D\,\frac{\partial^2y}{\partial r^2}+g(x,y,z)-k_fy&=0,\\ D\,\frac{\partial^2z}{\partial r^2}+h(x,z)+k_f(z_r-z)&=0. \end{aligned}\tag{8}$$

The variables x, y, and z have been further scaled in the numerical work presented below by multiplying by 1000, 100, and 1000, respectively. Letting x, y, and z also represent these rescaled variables, the reaction kinetics equations become Eq. (9).

$$\begin{aligned} f(x,y,z)&=s[y/10-100xy+x(1-1000z/c)-1000qx^2],\\ g(x,y,z)&=(-y-1000xy+10fz)/s,\\ h(x,z)&=w[x(1-1000z/c)-z]. \end{aligned}\tag{9}$$

III. NUMERICAL RESULTS

The major bifurcation parameters in the well-mixed reaction kinetics given by Eq. (6) are k_5 and f. All results reported here are for the chemical parameters specified above with $k_5=0.10\,\mathrm{s^{-1}}$ and $f=0.43$, for which Eq. (6) is bistable, there being two stable and one unstable steady states. Bistability in the reaction kinetics seems to be necessary for appearance of the stable, spatially inhomogeneous concentration patterns described below in the spatially distributed,

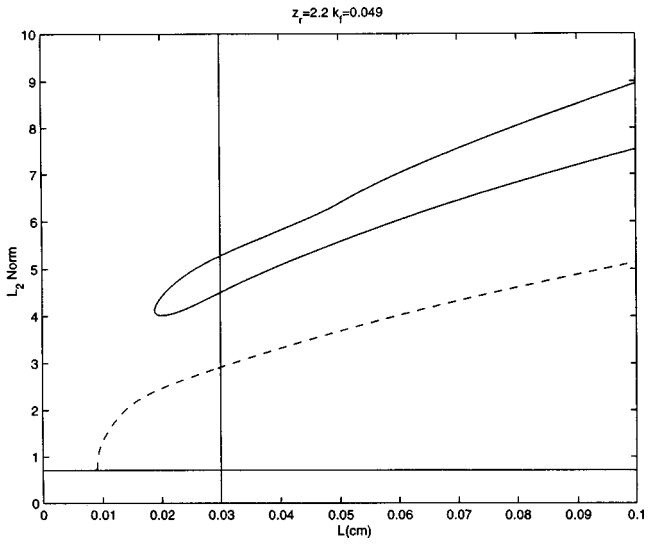

FIG. 2. L_2 norm of concentration for an unstable, spatially homogeneous solution and three stationary-pattern solutions to Eq. (8) obtained by continuation methods for $z_r=2.2$ and $k_f=0.049$ as the domain size L is varied. The lowest, solid line is the unstable, spatially homogeneous state, and the dashed line is the branch of unstable Turing patterns bifurcating from it. The two solid upper lines show a fold bifurcation at which a single spatially inhomogeneous (pattern) solution appears and immediately separates into two others, a fold bifurcation. The stability of the two highest-norm patterns is as indicated in Fig. 5. The vertical line indicates the value $L=0.3$ cm for which Fig. 3 is calculated.

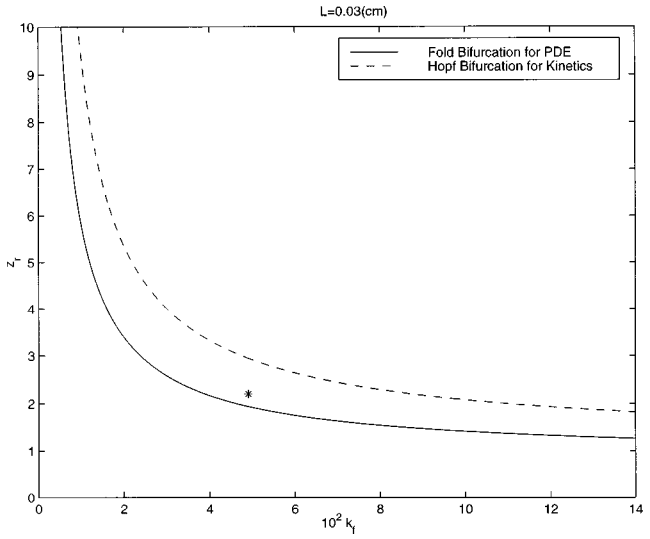

FIG. 3. Bifurcation structure of Eq. (8) in the $k_f - z_r$ plane at $L = 0.03$ cm. The solid line is the locus of points for which the fold bifurcation shown in Fig. 2 occurs. The dashed line is the locus of points for which the high x-low y steady state of Eq. (6) becomes unstable via a Hopf bifurcation. Equation (6) is bistable below and monostable above this line. The star indicates the point for which Fig. 2 is calculated.

reaction-diffusion system, Eq. (7), as has been found in previous closed system ($k_f = 0$) work with unequal diffusion coefficients [36,37]. This fact must guide experiments in the BZ system designed to verify the results obtained here.

Numerical investigation of Eq. (7) is begun using its time-independent form, Eq. (8). The physically important bifurcation parameters in the open system are k_f and z_r. Spatially inhomogeneous solutions are found and characterized for Eq.

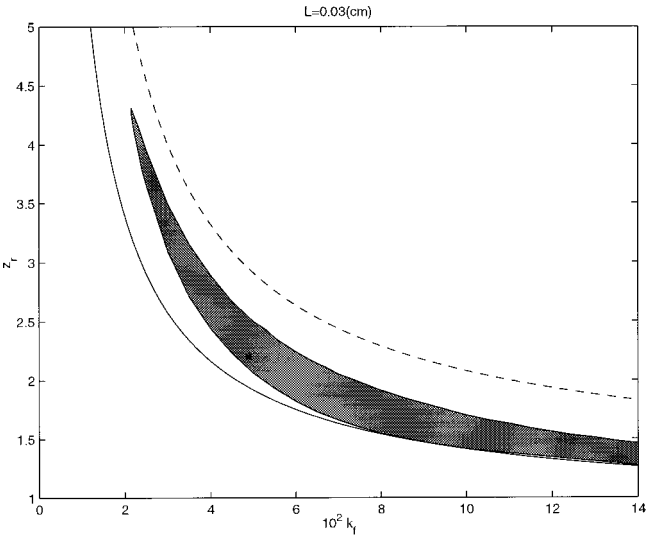

FIG. 4. Stability diagram in the $z_r - k_f$ plane for $L = 0.03$ cm resulting from linearization of Eq. (8) about spatially inhomogeneous solutions obtained by Newton's method. Stable, spatially inhomogeneous solutions are found only within the shaded region, whose boundary is a locus of points for which the linearized system has purely imaginary eigenvalues, indicating the possibility of a Hopf bifurcation in the full PDE system, Eq. (7). The Hopf and Fold bifurcation lines from Figs. 2 and 3 are reproduced.

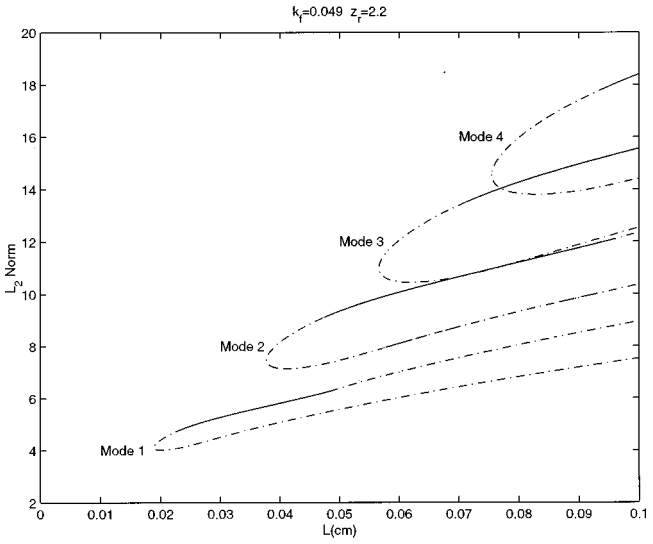

FIG. 5. Dependence on domain size, L, of the stability of four single and multilayer patterns for $k_f = 0.049$ and $z_r = 2.2$. Each curve is the Fold bifurcation as in Fig. 2 for two patterns having reflective symmetry, containing 1, 2, 3, or 4 layers, respectively, and growing from an instability of the form $\cos n\pi$ with n equal to 1, 2, 3, or 4. The lower pattern is unstable (dash-dot line) in all cases. The upper pattern in each case is stable (solid line) only over a certain range of domain length, which increases with the number of layers.

(8) in two ways. (i) Numerical continuation methods [42,43] are used to determine the existence of and to characterize spatially inhomogeneous steady state solutions to Eq. (8). (ii) Equation (8) is discretized using a second-order, central-difference method [41]. The resulting equations then are solved using Newton's method with a spatially inhomogeneous initial spatial distribution of x, y, and z. Equation (8) may then be linearized about the patterns so obtained and their stability as stationary solutions to Eq. (7) investigated. The results thus obtained are verified by numerical solution of Eq. (7) itself.

Figures 2 and 3 summarize the results of the continuation calculations based on Eq. (8). The existence and characteristics of spatial concentration patterns depend upon the values of L as well as k_f and z_r. There are three spatially uniform steady states for all physically reasonable, positive values of k_f and z_r. They correspond to the three steady states of Eq. (6). Two of these spatially uniform states for $k_f = 0$, those corresponding to the bistable high x-low y and the low x-high y states in the reaction kinetics, Eq. (6), are stable. The third state with intermediate values of x and y is always unstable. One, two, or three spatially inhomogeneous solutions also have been located. Figure 2 characterizes the existence of these solutions to Eq. (8) and their amplitude in the L_2 norm [44] as L varies and with $z_r = 2.2$ and $k_f = 0.049$. No spatially inhomogeneous solution is found for sufficiently small values of L. However, the steady state with intermediate values of x and y (the lowest solid line in Fig. 2) undergoes a classic Turing bifurcation [1,2] as L increases at which the homogeneous state becomes unstable relative to a cosinelike pattern that appears and grows in amplitude as L increases further. This is the dashed curve in Fig. 2. It can be shown that this pattern is unstable locally near the bifurca-

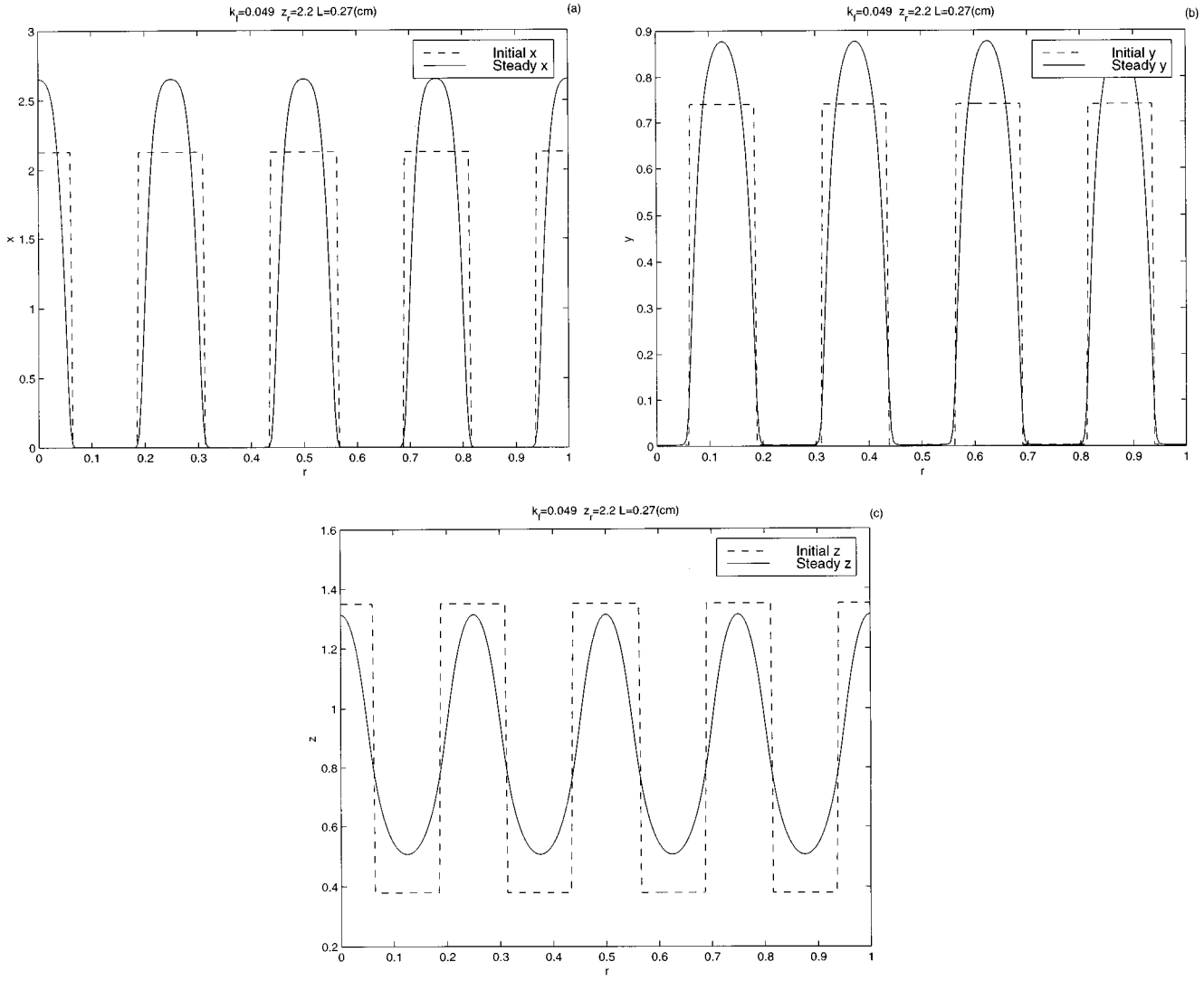

FIG. 6. Evolution of square-wave initial conditions (dashed line) to an eight-layer pattern (solid line) for $k_f=0.049$, $z_r=2.2$ and $L=0.27$ cm. (a) The value of x, (b) the value of y, (c) the value of z.

tion point because the spatially homogeneous solution it bifurcates from is unstable. We have found numerically that this branch of solutions is indeed unstable for all values of L, seeming to tend to an orbit homoclinic to the low x-high y, spatially homogeneous state as $L\rightarrow\infty$.

The fold bifurcation illustrated in Fig. 2 occurs at a somewhat higher value of $L=L_c$. A second spatially inhomogeneous solution appears and immediately separates into a pair of spatially inhomogeneous solutions as L increases beyond L_c. These states apparently are not associated with any spatially homogeneous state. Thus there are three pairs of spatially inhomogeneous solutions, each having reflective symmetry, at sufficiently large values of L, e.g., at $L=0.03$ cm, as indicated by the vertical line in Fig. 2. All solutions for this value of L are found in the Newton's method calculations to be single-layer patterns containing one-half of a concentration peak similar to one-half cosine wave. With Neumann boundary conditions, if $x(r)$, $y(r)$, $z(r)$ is a solution, then so is $x(L-r)$, $y(L-r)$, $z(L-r)$. These two patterns are counted as one. Similar symmetry is observed in multilayer patterns appearing at larger values of L.

The upper branch of the pair of spatially inhomogeneous solutions resulting from the fold bifurcation seems to tend to a heteroclinic orbit between the high x-low y and the low x-high y spatially uniform states as $L\rightarrow\infty$. The lower branch seems to correspond to an orbit homoclinic to the high x-low y spatially uniform state as $L\rightarrow\infty$. Numerical results described below suggest that the lower solution is always unstable, while the upper solution is stable for appropriate values of L. The high x-low y and low x-high y, spatially homogeneous states continue to exist for these values of k_f and z_r but are only locally stable.

Figure 3 illustrates the bifurcation structure of Eq. (8) in the k_f-z_r plane with $L=0.03$ cm, the point indicated by the vertical line in Fig. 2. The star in Fig. 3 indicates the values of k_f and z_r for which Fig. 2 is constructed. The dashed (Hopf) line in Fig. 2 is the locus of points for which the high x-low y spatially homogeneous solution to Eq. (6) loses its stability via a Hopf bifurcation. Below this curve the well-stirred chemical kinetics, Eq. (6), is bistable and there are two solutions corresponding to locally stable, spatially uniform states. Detailed investigations were not carried out

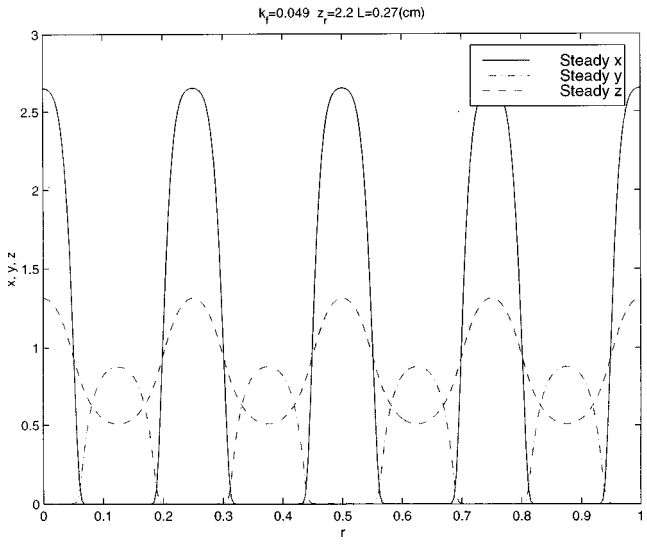

FIG. 7. Combined concentration profiles from Fig. 6.

above the Hopf curve where Eq. (6) has only one stable steady state. The Fold (solid) curve indicates the locus of points at which the turning point in Fig. 2 occurs. Two spatially inhomogeneous solutions, including the Turing solution, are present at this point. The region with three spatially inhomogeneous solutions (corresponding to Fig. 2 at L greater than L_c where the fold bifurcation occurs) lies between the Hopf and the Fold curves. Only the Turing solution exists below the Fold line. Spatially inhomogeneous patterns exist throughout the region bounded by the Hopf and the Fold lines. However, stable patterns are found only in a portion of this region.

The spatially inhomogeneous solutions located by continuation methods can be computed by solution of the spatially discretized version of Eq. (8) using Newton's method with iteration stopped when the residual is of the order of 10^{-10}. The stability of these solutions is investigated by computing the eigenvalues of the linearization of Eq. (8) about them. The EISPACK routines [45] as well as iterative techniques [46] are used to do this. The numerical results obtained indicate that the Fold lines in Figs. 2 and 3 result from a saddle-node bifurcation in which an eigenvalue of the linearization of Eq. (8) about the appropriate pattern is identically zero. These results are represented in Fig. 4, where the Hopf and Fold lines from Fig. 3 also are reproduced. Stable, spatially inhomogeneous solutions are found only within the shaded region between the Hopf and Fold curves. The boundary of this region is a curve of Hopf points for the linearization of the discretized version of Eq. (8) where the eigenvalues are purely imaginary. This indicates the possibility of a Hopf bifurcation for the PDE system, Eq. (7), such as occurs in analogous, closed-system activator-inhibitor models if the diffusion coefficient of the inhibitor is larger than that of the activator [47]. Temporally oscillatory, spatially inhomogeneous solutions referred to as breather patterns [47] may occur in this case close to the Hopf bifurcation. We describe below numerical breather solutions that are strong evidence for the existence of such a Hopf bifurcation in Eq. (7).

The existence and stability of spatially inhomogeneous solutions more complex than only a single-layer, i.e., multilayer patterns with more than one concentration peak, also has been investigated as a function of the domain length, L. These results are displayed in Fig. 5 for $0<L<0.1$ cm with $k_f=0.049$ and $z_r=2.2$. The fold bifurcation is again apparent, but the lower-amplitude, spatially inhomogeneous solution is always unstable. Patterns with one to four layers are found for $L\leqslant 0.1$ cm, but it appears that any number of layers can be obtained for large enough values of L. The L_2 norm of these patterns increases with the number of layers, indicating larger spatial concentration inhomogeneities. Each pattern is stable only in a range $L_0<L<L_1$ with the exchange of stability again seeming to be via a Hopf bifurcation and to be very regular in that if a single-layer pattern is stable in the range $L_0<L<L_1$, then the n-layer pattern is stable in the range $nL_0<L<nL_1$.

These results from continuation and stability analyses of the time-independent Eq. (8) are verified and extended by numerical solution of the PDE system, Eq. (7). The second-order spatial derivatives are discretized using second-order differences on a grid of n points. This results in a large system of $3n$ ordinary differential equations which are solved numerically using the stiffly stable numerical integrators ODE15S [48,49] and LSODE [50]. A spatial grid of 250 spatial points is normally used, but many calculations with 500 or 1000 points over the same spatial domain yield essentially identical results. It is assumed that a stable, unchanging solution has been achieved when the time derivatives are less than 10^{-10}. The stability of spatially inhomogeneous solutions to Eq. (8) obtained by Newton's method is verified by perturbing them by addition of 1% random noise before use as the initial condition for numerical solution of Eq. (7). All solutions for which the linearized version of the ODE Eq. (8) has a stable spectrum of eigenvalues are found to be numerically stable solutions to the PDE, Eq. (7).

We also have investigated numerically the evolution of initial square-wave initial concentration profiles given by Eq. (9) to apparently stable spatially inhomogeneous patterns,

$$x(r,0)=x_{r1}\ \max(\cos(\pi m r),0)+x_{r0}\ \max(\sin(\pi m r),0),$$

$$y(r,0)=y_{r1}\ \max(\cos(\pi m r),0)+x_{r0}\ \max(\sin(\pi m r),0),$$

$$z(r,0)=z_{r1}\ \max(\cos(\pi m r),0)+z_{r0}\ \max(\sin(\pi m r),0).$$

The parameters x_{r0} and x_{r1} are the respective values of x for the two steady states of the bistable reaction kinetics, Eq. (6), and similarly for y and z. Integration of Eq. (7) leads to a stable spatial pattern if the spatial interval, L, can support a pattern of wave number m. Figure 6 shows the initial and final concentration profiles for such a calculation for $m=4$ and with $L=0.27$ cm, $k_f=0.049$, and $z_r=2.2$. Figure 7 shows the complete eight-layer pattern, which is very similar to one found using the same model in a closed system ($k_f=0$), but with $D_z/(D_x=D_y)>2$. Thus it appears that differential transport of the inhibitor compared to the activator via exchange with the reservoir can substitute for differential transport via diffusion within the gel.

The previous indication of the existence of a Hopf bifurcation for the PDE system also can be investigated by numerical integration. Figure 8 shows the numerical evolution

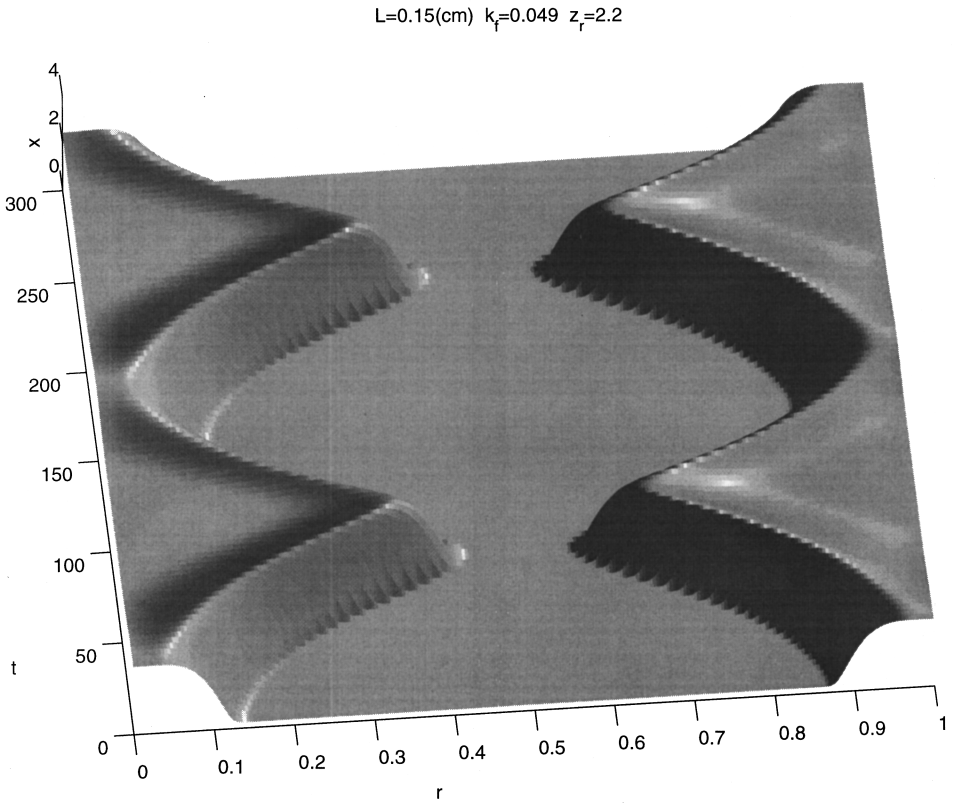

FIG. 8. Value of x vs r as dimensionless time, t, evolves for a two-layer breather solution with $k_f=0.049$, $z_r=2.2$, and $L=0.150$ cm. The value of L used is considerably above the bifurcation point indicated in Fig. 5 for Mode 2 in order to make the movement more apparent.

of Eq. (7) for a value of L past that where Hopf bifurcation occurs, L_H, as the domain length is increased. The two-layer initial concentration profile computed from Eq. (8) by Newton's method is unstable but does not decompose to a spatially homogeneous state. The profile instead behaves as two traveling waves that approach and move away from each other with a period of about 153 in dimensionless time units. This period agrees well with that computed from the eigenvalues obtained by linearization of Eq. (8), even though the value of L used in this calculation is considerably larger than L_H. This type of phenomenon has been investigated [47] in another activator-inhibitor system with $D_{\text{inhibitor}}/D_{\text{activator}}>1$ where the connection to the Hopf bifurcation can be shown precisely. This phenomenon may be related to small-amplitude, sinusoidal oscillations observed in a very similar well-mixed, CSTR model [35] near a Hopf bifurcation and to the formation of a stationary pattern in this model [37] with $k_f=0$ via the interaction and eventual stopping of traveling waves.

Stability analysis of the linearized version of Eq. (8) indicates that there likely is also a Hopf bifurcation as L is decreased. However, if there are periodic solutions near this change of stability such as occur (Fig. 8) for values of L beyond the high end of the range of pattern stability, then they must occur only over a very narrow range of L. Thus the stable, two-layer pattern that occurs for $k_f=0.049$, $z_r=2.2$, and $L=0.05$ cm becomes unstable for $L=0.04$ cm, evolving into two traveling waves that collide and eventually coalesce into the high x-low y, spatially homogeneous steady state, as is shown in Fig. 9.

The above results in one spatial dimension can be extrapolated to suggest the presence of a stable pattern in two spatial dimensions for $k_f=0.049$, $z_r=2.2$ on a square domain with $L=0.07$ cm. This pattern has been found using Newton's method and the two-dimensional version of Eq. (8). It is displayed in Fig. 10. The eigenvalue spectrum of this pattern computed via the iterative methods described above is stable.

IV. CONCLUSION

Solutions corresponding to stable, stationary, spatial concentration patterns exist to a set of reaction-diffusion equations arising from the Oregonator model of the BZ reaction. The physical configuration of the system modeled is an open, thin-layer, gelled reaction medium (Fig. 1) in contact with reservoirs over its two large surfaces, with which it exchanges various chemical species. These patterns are stable even when the diffusion coefficients of all reactive intermediates are equal. They are not a Turing structure [1] because they do not bifurcate from the spatially homogeneous state, they instead are isolated and must be reached via an appropriate perturbation of the spatially homogeneous state. So-called breather solutions also are found in which a spatial pattern persists indefinitely, but the size of the concentration inhomogeneities oscillates. They occur just outside the region of stability of the stationary patterns. Breathing patterns have been observed previously [51] in an enzyme-kinetics model and referred to there as pulsars. A breathing concentration inhomogeneity has been observed experimentally [52] in a gel-disc reactor with the pH-driven $Fe(CN)_6^{4-}$-IO_3^--SO_3^{2-} (FIS) chemical oscillator [53–55],

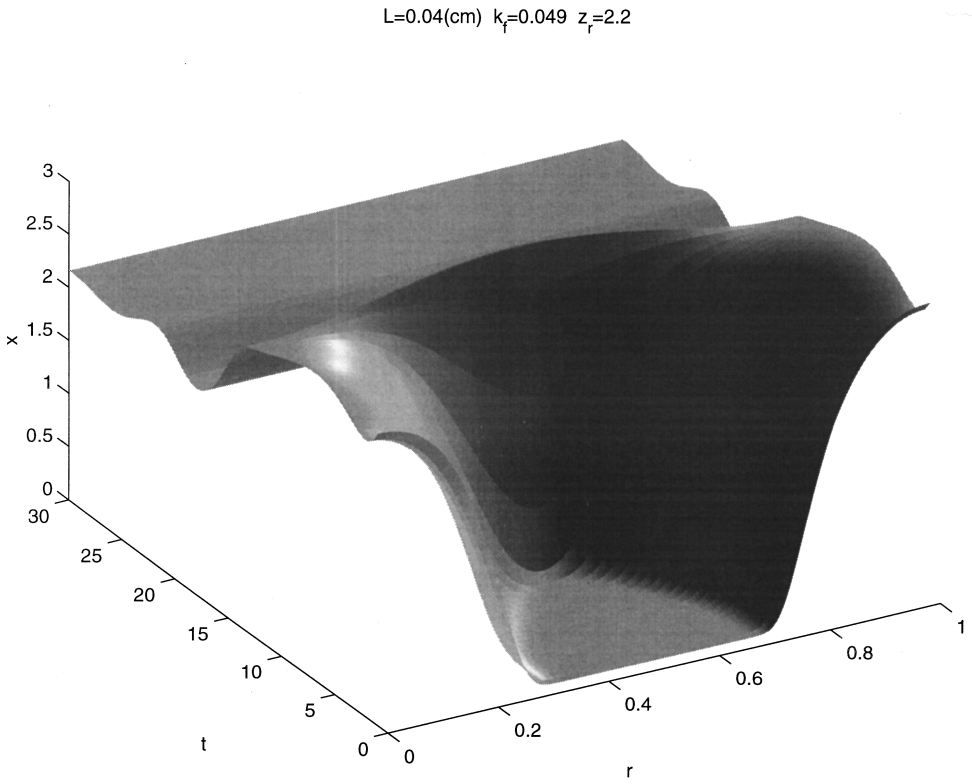

FIG. 9. Collapse in dimensionless time, t, of an unstable, two-layer pattern (x vs r) by collision of two traveling waves leading to a spatially homogeneous solution for $k_f = 0.049$, $z_r = 2.2$, and $L = 0.040$ cm. The value of L used is just below the bifurcation point indicated for Mode 2 in Fig. 5.

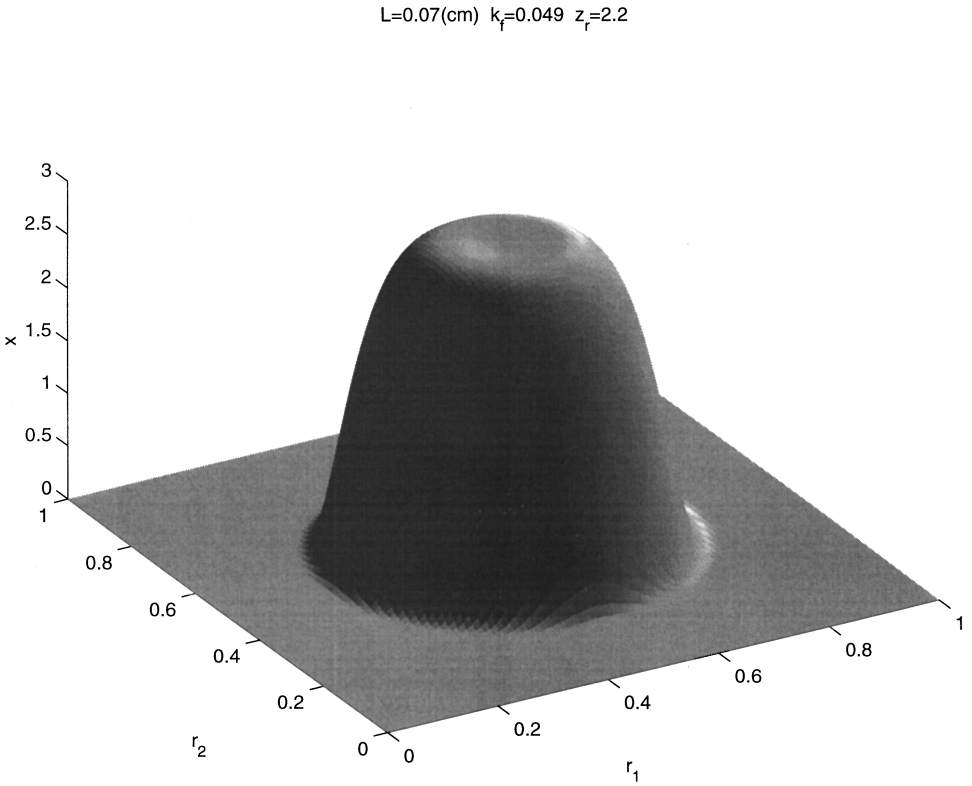

FIG. 10. Value of x for a stable two-dimensional pattern on a square domain with $L = 0.07$ cm, $k_f = 0.049$, and $z_r = 2.2$.

again apparently involving bistability [53] and near a bifurcation [52,56,57]. The high diffusivity of H^+ may allow for substantial differences of diffusion coefficients in the FIS system. The precise relationship of these observations to the present result is not yet established [56,57], especially concerning the exact bifurcation structure associated with the appearance of patterns, but there likely is a close relationship. There is an interesting interaction of traveling waves and stationary patterns in the FIS system [37,52,55], and some patterns are approached via a perturbation [55].

We believe that the patterns located here will appear in the BZ reaction under suitable experimental conditions. They are robust in our calculations and depend mainly upon the existence of bistability in the chemical kinetics, a phenomenon that is well-known in the BZ reaction [58]. Hale *et al.* [59] recently have reported very similar pattern-formation with all-equal diffusion coefficients for the cubic-autocatalator model [27,60] also dependent upon bistability and in the same open physical configuration, suggesting that the phenomenon is related to the existence of bistability in activator-inhibitor kinetics [52,53,56,57] in this physical configuration rather than to the exact form of the kinetic equations. We suggest that it will be necessary to carry out these experiments with bromomalonic acid as well as Ce(IV) in the reservoir(s) in order to control the effective value of f, assumed to be 0.43 in the present calculations. A more complex, eleven-variable model of the BZ reaction due to Györgyi *et al.* [35,61,62] and designed to reproduce the role of bromomalonic acid in the origin of chaos in the BZ reaction [63] has been quite successful [64] and would seem to be useful in locating the regions of bistability necessary for the appearance of these patterns. One would use this model in a simple approach to look for bistability in a well-mixed CSTR as the concentrations of the principal reactants in the CSTR and the concentrations of Ce(IV) and bromomalonic acid in the feed streams are varied. The calculations reported here would be reproduced with this model in a more complex approach to determining accurate experimental parameters. It will be necessary to reach the patterns described here by perturbation because of their isolation from the spatially homogeneous state. This most likely can be done photochemically [65].

Finally, this model, as pictured in Fig. 1, may have some significance to the process of channeling or other cooperative structural changes in a cell membrane [66]. It consists of a membrane in contact with reservoirs on either side, perhaps representing the inside and outside of the cell. The patterning could correspond to the appearance of channels through the membrane or to some other structural change, mediated by the concentration of some species, analogous to z_r, either inside or outside of the cell. Patterned and homogeneous spatial states coexist for suitable values of z_r, and the system can be perturbed from one state to the other by a spatially inhomogeneous perturbation, perhaps the binding to the membrane of an agonist, e.g., a ligand-gated channel [67]. Only the spatially homogeneous state will exist for other values of z_r, and the membrane then will not respond to such a perturbation with a cooperative structural change.

ACKNOWLEDGMENTS

The research of J.D.D. was supported in part by NSF Grant Nos. DMS-940416 and OSR-9350546. The research of R.J.F. was supported in part by the University of Montana and by NSF Grant No. OSR-9350546.

[1] A. M. Turing, Philos. Trans. R. Soc. London, Ser. B **327**, 37 (1952).
[2] J. D. Murray, *Mathematical Biology* (Springer-Verlag, New York, 1989).
[3] I. Lengyel and I. R. Epstein, Proc. Natl. Acad. Sci. USA **89**, 3977 (1992).
[4] G. Nicolis and I. Prigogine, *Self Organization in Chemical Systems* (Wiley-Interscience, New York, 1977).
[5] L. Segel and J. L. Jackson, J. Theor. Biol. **37**, 545 (1972).
[6] J. J. Tyson and H. Othmer, Prog. Theor. Biol. **5**, 1 (1978).
[7] *Chemical Waves and Patterns*, edited by R. Kapral and K. Showalter (Kluwer, Dordrecht, 1995).
[8] V. Castets, E. Dulos, J. Boissonade, and P. De Kepper, Phys. Rev. Lett. **64**, 2953 (1990).
[9] Q. Ouyang and H. L. Swinney, Nature (London) **352**, 610 (1991).
[10] I. R. Epstein and K. Showalter, J. Phys. Chem. **100**, 13 132 (1996).
[11] I. R. Epstein and I. Lengyel, Physica D **84**, 1 (1995).
[12] *Dynamism and Regulation in Nonlinear Chemical Systems*, edited by M. Marek, S. C. Müller, T. Yamaguchi, and K. Yoshikawa (Elsevier Science, Amsterdam, 1995).
[13] J. Boissonade, E. Dulos, and P. De Kepper, Understanding Chem. React. **10**, 221 (1995).
[14] I. Lengyel and I. R. Epstein, Acc. Chem. Res. **26**, 235 (1993).
[15] P. De Kepper, I. R. Epstein, K. Kustin, and M. Orbán, J. Phys. Chem. **86**, 170 (1982).
[16] I. Lengyel and I. R. Epstein, in *Chemical Waves and Patterns*, edited by R. Kapral and K. Showalter (Kluwer, Dordrecht, 1995), p. 297.
[17] P. De Kepper, V. Castets, E. Dulos, and J. Boissonade, Physica D **49**, 161 (1991).
[18] J. Boissonade, E. Dulos, and P. De Kepper, in *Chemical Waves and Patterns*, edited by R. Kapral and K. Showalter (Kluwer, Dordrecht, 1995).
[19] Q. Ouyang and H. Swinney, in *Chemical Waves and Patterns*, edited by R. Kapral and K. Showalter (Kluwer, Dordrecht, 1995); I. R. Epstein, I. Lengyel, S. Kádár, M. Kagan, and M. Yokoyama, Physica A **188**, 26 (1992).
[20] I. Lengyel, S. Kádár, and I. R. Epstein, Phys. Rev. Lett. **69**, 2729 (1992).
[21] E. Dulos, P. Davies, B. Rudovics, and P. De Kepper, Physica D **98**, 9 (1996).
[22] R. J. Field, E. Körös, and R. M. Noyes, J. Am. Chem. Soc. **94**, 8649 (1972).
[23] T. Turányi, L. Györgyi, and R. J. Field, J. Phys. Chem. **97**, 1931 (1993).
[24] L. Györgyi, T. Turányi, and R. J. Field, J. Phys. Chem. **94**, 7162 (1990).

[25] R. J. Field, in *Oscillations and Traveling Waves in Chemical Systems*, edited by R. J. Field and M. Burger (Wiley-Interscience, New York, 1985).
[26] R. J. Field and F. W. Schneider, J. Chem. Educ. **66**, 195 (1989).
[27] P. Gray and S. K. Scott, *Chemical Oscillations and Instabilities* (Oxford University Press, Oxford, 1990).
[28] A. N. Zaikin and A. M. Zhabotinsky, Nature (London) **225**, 535 (1972).
[29] A. T. Winfree, *When Time Breaks Down* (Princeton University Press, Princeton, 1987).
[30] S. C. Müller and T. Plesser, in *Chemical Waves and Patterns*, edited by R. Kapral and K. Showalter (Kluwer, Dordrecht, 1995).
[31] *Waves and Patterns in Chemical and Biological Media*, edited by H. L. Swinney and V. I. Krinsky (North-Holland, Amsterdam, 1991) [reprinted from Physica D **49D**, 1 (1991)].
[32] A. T. Winfree, SIAM (Soc. Ind. Appl. Math.) Rev. **32**, 1 (1990).
[33] P. De Kepper, J.-J. Perraud, B. Rudovics, and E. Dulos, World Sci. Ser. Nonlin. Sci. B **3**, 147 (1995).
[34] R. J. Field and R. M. Noyes, J. Chem. Phys. **60**, 1877 (1974).
[35] L. Györgyi and R. J. Field, Nature (London) **355**, 808 (1992).
[36] P. K. Becker and R. J. Field, J. Phys. Chem. **89**, 118 (1985).
[37] A. L. Kawczynski, W. S. Comstock, and R. J. Field, Physica D **54**, 220 (1991).
[38] J. Guslander and R. J. Field, J. Phys. Chem. **96**, 10 575 (1992).
[39] A. Nomura, H. Miike, and T. Sakurai, J. Phys. Soc. Jpn. **66**, 598 (1997).
[40] J. J. Tyson, in *Oscillations and Traveling Waves in Chemical Systems*, edited by R. J. Field and M. Burger (Wiley-Interscience, New York, 1985).
[41] W. H. Press, B. R. Flannery, S. A. Teukolsky, and W. T. Vettering, *Numerical Recipes* (Cambridge University Press, Cambridge, 1986), Chap. 17.
[42] E. J. Doedel and J. P. Kernevez, California Institute of Technology Applied Mathematics Report, 1986.
[43] E. L. Allgower and K. Georg, *Numerical Continuation Methods: An Introduction* (Springer-Verlag, New York, 1990).
[44] $L_2=\sqrt{\int_0^1(\partial x/\partial r)^2dr+\int_0^1(\partial y/\partial r)^2dr+\int_0^1(\partial z/\partial r)^2dr}$.
[45] B. T. Smith, J. M. Boyle, J. J. Dongarva, B. S. Garbow, Y. Ikebe, V. C. Klema, and C. B. Moler, *Matrix Eigensystem Routines–EISPACK Guide XI*, Lecture Notes in Computer Science, 2nd ed. (Springer-Verlag, New York, 1976), Vol. 6.
[46] K. Meerbergen, A. Spence, and D. Roose, BIT Numerical Math. **34**, 409 (1994).
[47] Y. Nishiura and M. Mimura, SIAM (Soc. Ind. Appl. Math.) J. Appl. Math. **49**, 481 (1989).
[48] L. F. Shampine and M. W. Reichelt, SIAM J. Sci. Comp. (to be published).
[49] U. M. Ascher, S. J. Ruuth, and B. T. R. Wetton, SIAM (Soc. Ind. Appl. Math.) J. Numer. Anal. **32**, 797 (1995).
[50] A. C. Hindmarsh, ODEPACK, A Systematized Collection of ODE Solvers, Lawrence-Livermore National Laboratory Report No. UCRL-88007 (1982).
[51] A. L. Kawczynski, J. Non-Equilib. Thermodyn. **3**, 29 (1979); Polish J. Chem. **57**, 1323 (1983).
[52] G. Li, Q. Ouyang, and H. L. Swinney, J. Chem. Phys. **105**, 10 830 (1996).
[53] E. C. Edblom, M. Orbán, and I. R. Epstein, J. Am. Chem. Soc. **108**, 2826 (1986).
[54] K. J. Lee, W. D. McCormick, Q. Ouyang, and H. L. Swinney, Science **261**, 192 (1993); K. J. Lee, W. D. McCormick, J. E. Pearson, and H. L. Swinney, Nature (London) **369**, 215 (1994).
[55] K. J. Lee and H. L. Swinney, Phys. Rev. E **51**, 1899 (1995).
[56] A. Hagberg and E. Meron, Phys. Rev. E **48**, 725 (1993); A. Hagberg and E. Meron, Phys. Rev. Lett. **72**, 2494 (1994); A. Hagberg and E. Meron, Chaos **4**, 477 (1994); C. Elphick, A. Hagberg, and E. Meron, Phys. Rev. E **51**, 3052 (1995).
[57] A. Hagberg, E. Meron, I. Rubenstein, and B. Zaltzman, Phys. Rev. Lett. **76**, 427 (1996).
[58] P. De Kepper and J. Boissonade, J. Chem. Phys. **75**, 189 (1981).
[59] J. K. Hale, L. A. Pelletier, and W. C. Troy (unpublished).
[60] S. K. Scott, *Oscillation, Waves and Chaos in Chemical Kinetics* (Oxford University Press, Oxford, 1994), Chap. 5; S. K. Scott, Acc. Chem. Res. **20**, 186 (1987).
[61] L. Györgyi, S. Rempe, and R. J. Field, J. Phys. Chem. **95**, 3159 (1991).
[62] L. Györgyi and R. J. Field, J. Phys. Chem. **95**, 6594 (1991).
[63] L. Györgyi, R. J. Field, Z. Noszticzius, W. D. McCormick, and H. L. Swinney, J. Phys. Chem. **96**, 1228 (1992).
[64] F. W. Schneider, R. Bittersdorf, A. Förster, T. Hauck, D. Lebender, and J. Müller, J. Phys. Chem. **97**, 12 244 (1993); M. Kraus, J. Müller, D. Lebender, and F. W. Schneider, Chem. Phys. Lett. **51**, 260 (1996).
[65] P. G. Sørensen, T. Lorenzen, and F. Hynne, J. Phys. Chem. **100**, 19 192 (1996).
[66] B. Hille, *Ionic Channels of Excitable Membranes*, 2nd ed. (Sinauer Associates, Inc., Sunderland, MA, 1992).
[67] B. Hille, *Ionic Channels of Excitable Membranes* (Ref. [66]), Chap. 6.